

Published in final edited form as:

Biochemistry. 2011 September 6; 50(35): 7476–7483. doi:10.1021/bi2009739.

Pericyclic reactions catalyzed by chorismate-utilizing enzymes

Audrey L. Lamb[†]

Department of Molecular Biosciences, University of Kansas, Lawrence, Kansas 66045

Abstract

One of the fundamental questions of enzymology is how catalytic power is derived. This review focuses on recent developments in the structure-function relationships of chorismate-utilizing enzymes involved in siderophore biosynthesis to provide insight into the biocatalysis of pericyclic reactions. Specifically, salicylate synthesis by the two-enzyme pathway in *Pseudomonas aeruginosa* is examined. The isochorismate-pyruvate lyase is discussed in the context of its homologues, the chorismate mutases, and the isochorismate synthase is compared to its homologues in the MST-family (menaquinone, siderophore or tryptophan biosynthesis) of enzymes. The tentative conclusion is that the activities observed cannot be reconciled by inspection of the active site participants alone. Instead, individual activities must arise from unique dynamic properties of each enzyme that are tuned to promote specific chemistries.

Siderophores are low molecular weight iron chelators produced by bacteria, fungi and plants, which scavenge iron from the environment, and are frequently required for virulence in pathogenic bacteria (1, 2). The isochorismate synthase (PchA) and isochorismate-pyruvate lyase (PchB) from *Pseudomonas aeruginosa* are involved in the synthesis of the siderophore pyochelin (3, 4). PchA converts chorismate to isochorismate which PchB in turn uses to produce salicylate by elimination of pyruvate. These enzymes will be used as the basis for a discussion of enzymatically-catalyzed pericyclic reactions. It is useful to consider these enzymes in the reverse order of the biosynthetic pathway.

Reactions Catalyzed by PchB

PchB catalyzes chiefly the *pericyclic* reaction of Figure 1A. A pericyclic reaction is a concerted one in which a closed, cyclic flow of electrons (curved arrows) leads from bound reactants to bound products. For PchB, the reaction is a concerted but asynchronous [1,5]-sigmatropic shift with a quantitative hydrogen transfer from C2 to C9 as detected by NMR (5) and confirmed computationally (6), with an observed k_{cat}/K_m of $4.11 \times 10^4 \text{ M}^{-1} \text{ s}^{-1}$ (7). Interestingly, PchB can also perform a nonphysiological role as a chorismate mutase (Figure 1B), albeit with considerably lower catalytic efficiency (3) ($k_{cat}/K_m = 1.96 \times 10^2 \text{ M}^{-1} \text{ s}^{-1}$ (7)). This reaction, also pericyclic, is a Claisen rearrangement of chorismate to prephenate in which the concerted but asynchronous [3,3]-sigmatropic shift transfers the pyruvate tail from the C3 ether linkage to a C1–C9 linkage (8). Therefore, PchB catalyzes *two* pericyclic reactions, which are unusual in biology.

Pericyclic reactions are attractive for study as examples of fundamental enzyme theory since the reaction catalyzed does not require direct contribution from the enzyme. For example, no protons or electrons are donated or accepted from the enzyme or cofactors, nor are there

[†]This publication was made possible by funds from NIH grant number P20 RR016475 from the INBRE Program of the National Center for Research Resources, and by NIH grants numbered R01 AI77725 and K02 AI093675 from the National Institute for Allergy and Infectious Disease.

corresponding author; phone: (785)864-5075; fax: (785)864-5294; lamb@ku.edu.

covalent intermediates. Instead, the binding event leads to organization of the substrate into the transition state thereby resulting in product formation. However, this also means that pericyclic reactions present problems for use of many traditional ideas about enzyme catalysis, since the concepts from acid-base, metal-ion and covalent catalysis do not apply. Electrostatic stabilization is also problematic: the reactions are concerted in the sense that there are no intermediate compounds formed, but the cyclic electron distribution of the transition state is still an unsettled issue; i.e. the charge distribution in the transition state may be debatable. Nevertheless, the enzymes that perform these reactions, especially the chorismate mutases, have been studied in detail to develop fundamental ideas of transition state theory and more generally catalysis.

PchB is a structural homolog of the AroQ chorismate mutases

Sequence similarity (20%) between PchB and the chorismate mutases of the AroQ structural class led to the hypothesis that PchB is a structural homologue of *E. coli* chorismate mutase (EcCM) (3). Three structures of wildtype PchB have been published (9, 10) and these indicate that PchB is indeed a structural homologue of EcCM (Figure 2). In the structure of EcCM, an oxabicyclic transition state analogue is held in place by interaction with a total of eight charged/polar amino acids (11). In PchB, however, only five of those amino acids are conserved, and the decreased number of hydrogen bonds and ionic interactions may lead to known promiscuity of this enzyme and the ability to catalyze both the lyase and mutase reactions (Figure 3) (10). There is a major structural difference between the apo-form and the pyruvate-bound or the pyruvate-and-salicylate-bound forms of PchB: the active site loop between helix one and helix two is disordered in the apo-structure but fully ordered in the ligand-bound structures. A difference between the open and closed structures is due to a conserved active site lysine (residue 42, green in Figure 3) which hydrogen bonds to a bound pyruvate molecule. These structures may represent an open state for substrate or product entry and egress and a closed catalytic state (10).

Structures of the chorismate mutases

The chorismate mutases of the AroQ class, such as EcCM, comprise an intertwined dimer composed of three helices (Figure 2). The two equivalent active sites per dimer are buried, and formed from amino acids from both monomers. In the only EcCM structure determined, a transition state analogue (TSA) is aligned in the active site by interaction of its carboxylates with arginines, one from each monomer (11). A debate has arisen in the field about how EcCM ($k_{\text{cat}}/K_{\text{m}}$ of $2.4 \times 10^5 \text{ M}^{-1}\text{s}^{-1}$, (12)) derives its catalytic power, and this debate has consistently cited work on the chorismate mutase from *Bacillus subtilis* (BsCM; $k_{\text{cat}}/K_{\text{m}}$ of $1 \times 10^6 \text{ M}^{-1}\text{s}^{-1}$ (13)). The data derived from EcCM and BsCM are sometimes compared directly even though the proteins are not structurally homologous. BsCM, an AroH chorismate mutase, is a trimer that forms a pseudo α/β -barrel with active sites at the interfaces between the monomers (Figure 2). The structure of BsCM has been determined apo-, with prephenate-bound, and with TSA-bound (14–16); however, there is little difference in the active sites of the three structures. In BsCM, the product/TSA is oriented in the active site by comparable arginines to those in the EcCM. Again, the active sites of EcCM and BsCM are usually considered comparable due to their shape and charge complementarity (17).

Hilvert and colleagues have developed a monomeric AroQ chorismate mutase by inserting an eight amino acid hinge-loop sequence into helix one, which allows this helix to fold over to form a shortened coiled-coil that is the structural basis of the protein and also allows for completion of the active site (18–20). This engineered monomeric *Methanococcus jannaschii* chorismate mutase (mMjCM) has comparable kinetic parameters ($k_{\text{cat}}/K_{\text{m}}$ of 1.9

$\times 10^4 \text{ M}^{-1}\text{s}^{-1}$) to that of the wildtype MjCM ($k_{\text{cat}}/K_{\text{m}}$ of $6.4 \times 10^4 \text{ M}^{-1}\text{s}^{-1}$) and the EcCM under similar conditions ($k_{\text{cat}}/K_{\text{m}}$ of $3.0 \times 10^4 \text{ M}^{-1}\text{s}^{-1}$) (18). Yet, mMjCM is molten globule in the absence of ligand, but forms the structure seen in Figure 2 in the presence of the oxabicyclic transition state analogue (19, 20).

Chorismate mutases: catalytic power

One hypothesis to explain how chorismate mutases derive their catalytic power is electrostatic transition state stabilization (TSS). Considerable biochemical data support this hypothesis, and indicate that a positively charged amino acid (Lys39 in EcCM, Arg90 in BsCM) stabilizes the developing negative charge during bond breaking at the ether oxygen (8, 12, 13, 21–23). Mutational analysis in EcCM (Lys39) and BsCM (Arg90) have determined this site to be critical for catalysis (12, 13). The conservative change in BsCM of Arg90 to a citrulline (isoteric but neutral) or to lysine (similarly positively charged), decreases the catalytic efficiency by at least three orders of magnitude, whereas deletion of the sidechain (R90A) led to a complete abolition of activity (13, 23). Similar mutations in EcCM (for example, K39A) lead to a decrease in $k_{\text{cat}}/K_{\text{m}}$ of five orders of magnitude (12). A critique of the mutagenesis work in the chorismate mutases is that mutagenesis at this lysine in EcCM alters the active site to an extent that the absence or presence of a positively charged amino acid at this site is immaterial (24). The evidence for this comes from a shoulder at $\sim 210 \text{ nm}$ in the circular dichroism spectra (12).

A second hypothesis has a basis in quantum mechanical/molecular mechanical molecular dynamics simulations (QM/MM-MD): formation of a near attack conformation (NAC) (24–29). A NAC is defined as a structure in which the reacting atoms are within van der Waals contact distance and approach at an angle $\pm 15^\circ$ to the bond that is formed, or an orientation in which the π -orbitals overlap (Figure 1) (25, 27). While a NAC is a “turnstile” through which reactants pass on the way to the transition state (27), once a NAC is formed, the reaction occurs spontaneously without further electrostatic stabilization or steric strain (24–27, 29). Interestingly, the mutase reaction and elimination of the enolpyruvyl sidechain are both observed in the uncatalyzed reaction (30, 31). However, the elimination reaction is not catalyzed by the chorismate mutase enzymes. Therefore, formation of the NAC for the Claisen rearrangement does not lead to the transition state for the elimination reaction (27). In other words, in an aqueous environment, it is possible to form a variety of NACs that proceed through different transition states to produce different products. Chorismate mutases limit the type of NACs formed, and catalysis proceeds through a particular transition state to form the desired product. In this model, formation of the reactive conformation of the substrate is the prerequisite for the enzyme to be a catalyst (24–27, 29).

QM/MM calculations at very high levels of QM theory have found that catalysis is due to a combination of transition state stabilization and conformational effects for BsCM (32). The substrate binds in the active site as a NAC according to all proposed definitions, but formation of this bound conformation is not the sole source of catalytic power. Instead, a combination of binding the reactive conformation and electrostatic transition state stabilization provides the decrease in the energy barrier for catalysis (33–35). Recent benchmark calculations by Dr. Mulholland's group using high-level *ab initio* QM/MM methods give results in excellent agreement with experiment for the activation enthalpies and free energies of the BsCM reaction (32).

Catalysis by the PchB is dependent on the 42 site

Whereas it is likely that PchB will perform the mutase reaction using a mechanism similar to that seen for its structural homologue EcCM, it is unlikely that PchB will use the same mechanism to perform the physiologically important lyase reaction. More to the point, the

two reactions must have differing near attack conformations and/or transition states (Figure 1), suggesting differing reaction mechanisms. Mutational analysis of PchB has led to insight into the alternative reaction mechanisms for the two reactions catalyzed by this enzyme (7). Importantly, mutation of the lysine at the 42 position (green in Figure 3) that is comparable to the lysine hypothesized to be important in electrostatic transition state stabilization in EcCM did not lead to structural perturbation of the active site. Evidence for this is provided in the form of circular dichroism data (7), and also the x-ray structures of the K42A (7) and K42E (9) mutants. However, K42A-PchB showed 1% of WT mutase and lyase activities, whereas the K42E mutant had no detectable activity for either reaction (7). Furthermore, examination of the effects of a variety of active site variants provides experimental evidence in agreement with the QM/MM calculations that suggest that neither a reactive substrate conformation nor electrostatic transition state stabilization completely accounts for k_{cat} of the rate-determining step for the two catalyzed reactions (7).

An intriguing result comes from pH profiles of the K42H mutant: k_{cat} is titrated with changing pH indicating that a positive charge at the 42 is necessary for efficient catalysis. It should be noted that this variant form retains the ability to catalyze the lyase reaction when the sidechain is deprotonated (~100-fold decrease in k_{cat}/K_M), indicating that the enzyme is a sufficient catalyst even without this sidechain charge (9). A calculation of an experimental $\Delta\Delta G^\ddagger$ by comparing the mutational effect at low and high pH gives a value of 2.4 kcal/mol for electrostatic transition state stabilization at the 42 site. Temperature dependence of k_{cat} experiments indicate the difference in $\Delta\Delta G^\ddagger$ between the uncatalyzed and enzyme-catalyzed lyase reaction is 7.43 kcal/mol, and there is a large entropic penalty for the transition from the enzyme-substrate complex to the transition state (36). One plausible explanation is that loop closing occurs after the initial binding event and may, with the positively charged amino acid at the 42 site, drive the formation of the transition state. This is in agreement with the pre-steady state kinetic experiments for mMjCM which indicate that conformational ordering is on the same timescale as catalysis, suggesting that conformational plasticity is linked to efficient enzymatic catalysis (19).

PchB is unusual in siderophore biosynthesis

Several bacterial species incorporate salicylate into their siderophores (Figure 4). The formation of yersiniabactin by *Yersinia enterocolitica* and mycobactin by *Mycobacterium tuberculosis* requires the conversion of chorismate to salicylate which is accomplished by a single enzyme (Irp9 and MbtI, respectively) in a single active site (37–40) (Figure 5). The salicylate synthases convert chorismate to salicylate via the formation of an isochorismate intermediate by general acid/general base catalysis, followed by a pericyclic reaction to generate salicylate, which is analogous to that catalyzed by PchB. The isochorismate synthases from *Escherichia coli* (EntC and MenF) and *Pseudomonas aeruginosa* (PchA) are homologues of the salicylate synthases (41–43). PchA produces isochorismate for conversion to salicylate by PchB and incorporation into the pyochelin siderophore. EntC is part of the enterobactin biosynthetic pathway, forming a dihydroxybenzoate-capped siderophore (44, 45) and MenF produces isochorismate as the first step in the biosynthesis of the electron carrier menaquinone (46). Whereas these enzymes are hypothesized to perform analogous general acid/general base chemistry to produce isochorismate as observed for MbtI and Irp9, they do not perform the pericyclic reaction to produce salicylate. This means that PchA, MenF and EntC cannot perform any pericyclic reactions despite homology to enzymes that can: Irp9 and MbtI. Most intriguingly, the two bi-functional enzymes do not have a PchB-like domain, but are able to perform the lyase activity with the structurally and functionally homologous domain found in MenF and EntC.

Structures of the enzymes that synthesize isochorismate (MST enzymes)

The x-ray crystallographic structures of four enzymes that isomerize chorismate to isochorismate have been determined (37, 38, 40–43). Irp9, MbtI, MenF and EntC are structural homologues (PchA awaits structure determination for confirmation of this hypothesis), with an α - β fold first described for the TrpE subdomain of anthranilate synthase (Figure 6) (47). These enzymes belong to a family of enzymes involved in menaquinone, siderophore or tryptophan biosynthesis and collectively have been named the MST family (40). The catalytic mechanism for isomerization of the chorismate ring has been determined through the cumulative work of several groups by structural and mutational analyses (38, 40, 41). A Mg^{2+} ion in the active site orients the C1 carboxyl group of chorismate. A lysine residue serves as a general base for the activation of water to attack at the C2 carbon, and a glutamic acid is a general acid for elimination of the C4-OH (Table 1 and Figure 7). However, recent work by Ziebart and Toney indicates that activation of water as a nucleophile may not be solely attributable to Lys147/205 of EntC/MbtI as K→Q mutations retained some activity (48). The catalytic mechanism for conversion of isochorismate to salicylate by MbtI has been shown to be a sigmatropic, pericyclic mechanism by analogous experiments to those described above for PchB (40). This reaction is pH dependent, occurring only at pH values 7.5 and greater (40). Chorismate mutase activity has also been detected in MbtI with a k_{cat}/K_m value approximately one third that of the salicylate synthase activity, using protein purified in two different ways, using a histidine-tag or an intein-chitin-tag (40). In these experiments, whereas salicylate synthase activity is Mg^{2+} dependent, the chorismate mutase activity was only detected when the Mg^{2+} was not present in the wildtype active site. MbtI has also been purified with a histidine tag and a second ion exchange step to produce a sample that has reduced or no detectable chorismate mutase activity, and the authors suggest that the mutase activity is the result of a contaminant (48). Keeping in mind the contrary evidence, MbtI may perform two pericyclic reactions. If so, the active site must be altered by the removal of the Mg^{2+} cofactor for the adventitious chorismate mutase catalysis, implying differing binding modes for the chorismate which lead to differing reactive substrate conformations and/or transition states and thus different products.

Presumably, the homologues that are lyase-active salicylate synthases must have structural features that the lyase-deficient isochorismate synthases do not. Whether this would be an amino acid for electrostatic stabilization of the transition state or an active site that selects for or arranges the substrate into a near attack conformation is still an open question. A close examination of the active sites leads to the startling realization that all but three of the amino acids are strictly conserved (Table 1 and Figure 7). First, EntC has a phenylalanine in place of a tyrosine (all other homologues) at one location in the active site (residue 327). Mutation at this site decreased isochorismate synthase activity by more than an order of magnitude, but did not lead to detectable salicylate production (43). Second, the backbone carbonyl of T348 in Irp9 H-bonds to the salicylate-OH, and this amino acid is conserved in MbtI. The transition of this amino acid from Thr to Ala is a conserved change for the enzymes that are lyase deficient (MenF, EntC and PchA). It has been proposed that this amino acid is responsible for the differences in activities of the two groups of enzymes (lyase-active and lyase-deficient). However, mutation of A to T at this site in both MenF (41) and EntC (43) did not convert these enzymes to lyase-active: neither variant enzyme produced salicylate and both showed significant decreases in their physiological isochorismate synthase activity. Finally, a trend can also be detected between lyase-active and lyase-deficient homologues at a residue that chelates the Mg^{2+} through a water molecule. In Irp9 and MbtI, the lyase-active enzymes, this amino acid is a glutamic acid (E281 and E294, respectively; see Table 1). However, the lyase-deficient homologues (MenF, EntC, and PchA) all have an amino acid that is one methylene group shorter, either an aspartic acid (EntC and PchA) or an

asparagine (MenF). This site has largely been ignored in the literature, probably because of its distance from the site of chemistry. Nevertheless, as shown in the stereo diagram (Figure 7), this difference in sidechain length may cause a shift in the binding of the Mg^{2+} and thus select for the products formed in the active site. It is tempting to propose that this shift may result in the inability to make a reactive substrate conformation in the lyase-deficient enzymes, but this hypothesis awaits testing.

Alternate reaction pathways and the free-energy landscape

In this paper, we have discussed three of the folds that catalyze two pericyclic reactions and the analysis illustrates that sequence and structural homology do not correlate to catalytic predictability: 1) structural homologues with strong sequence conservation at the active site may or may not have pyruvate-lyase activity (the salicylate and isochorismate synthases), 2) structural homologues with low conservation of active site residues catalyze one or two pericyclic reactions (*E. coli* chorismate mutase and the isochorismate-pyruvate lyase; respectively), and 3) enzymes with differing folds perform the same chemistry (*E. coli* and *B. subtilis* chorismate mutases). The pericyclic reactions catalyzed in this discussion are single substrate, and require no participation from the enzyme in the form of general acid-general base chemistry, metal ion catalysis (the Mg^{2+} of the MST enzymes are structural, orienting the substrate), or a covalent intermediate. Let us assume that the requirements for an active site that efficiently catalyzes one or more pericyclic reactions are: the ability to force the substrate into a reactive conformation with the pyruvylenol tail over the ring, and/or to have a strategically placed positive amino acid to stabilize the developing negative charge of the transition state. In other words, the ability of the different enzymes to perform zero, one or two pericyclic reactions may be conferred by simple positional interaction strategies. However, many changes to the first and second tier amino acids of the active sites of these enzymes have been made rationally and by directed evolution with minimal success (43, 49, 50) strongly suggesting that simple structural correlations are insufficient to account for the observed chemistries.

The laboratory-evolved mMjCM which orders upon ligand binding (18–20) is suggestive of the idea that catalytic power may be derived from the ability of these enzyme active sites to develop a “catalytic network” as described by Benkovic, Hammes and Hammes-Schiffer (51). While these authors weren’t considering protein folding from a molten globule, they do suggest that catalysis must be considered in the context of protein motion, including large conformational modes such as changes elicited by binding of ligands and vibrational modes on the timescale of catalysis (51). A three dimensional free energy landscape with many possible alternate reaction paths which are occupied by multiple sequential intermediates allow for the generally similar yet subtly different active sites to be (or not to be) catalysts. The differing pathways traveled by the substrate-enzyme ensemble along the mountain ranges of the free energy landscape may require differing relative contributions of the near attack conformation or electrostatic transition state stabilization.

Abbreviations and Full Textual Notes

AroH	protein family with sequence homology to chorismate mutases with α/β -barrel fold
AroQ	protein family with sequence homology to chorismate mutases with all α -helical fold
BsCM	<i>Bacillus subtilis</i> chorismate mutase
EcCM	<i>E. coli</i> chorismate mutase

EntC	isochorismate synthase from <i>E. coli</i>
Irp9	salicylate synthase from <i>Yersinia enterocolitica</i>
NAC	near attack conformation
MbtI	salicylate synthase from <i>Mycobacterium tuberculosis</i>
MenF	isochorismate synthase from <i>E. coli</i>
mMjCM	laboratory derived monomeric chorismate mutase from <i>Methanococcus jannaschii</i>
MST	protein family containing proteins of menaquinone, siderophore or tryptophan biosynthesis
PchA	isochorismate synthase from <i>Pseudomonas aeruginosa</i>
PchB	isochorismate-pyruvate lyase from <i>Pseudomonas aeruginosa</i>
QM/MM-MD	quantum mechanical/molecular mechanical molecular dynamics simulations
TS	transition state
TSA	transition state analogue
TSS	transition state stabilization

Acknowledgments

I am grateful to Drs. R. H. Himes and R. L. Schowen for critically reading this manuscript.

References

1. Sandy M, Butler A. Microbial iron acquisition: marine and terrestrial siderophores. *Chem Rev.* 2009; 109:4580–4595. [PubMed: 19772347]
2. Schalk IJ. Metal trafficking via siderophores in Gram-negative bacteria: specificities and characteristics of the pyoverdine pathway. *J. Inorg. Biochem.* 2008; 102:1159–1169. [PubMed: 18221784]
3. Gaille C, Kast P, Haas D. Salicylate biosynthesis in *Pseudomonas aeruginosa*. Purification and characterization of PchB, a novel bifunctional enzyme displaying isochorismate pyruvate-lyase and chorismate mutase activities. *J. Biol. Chem.* 2002; 277:21768–21775. [PubMed: 11937513]
4. Gaille C, Reimann C, Haas D. Isochorismate synthase (PchA), the first and rate-limiting enzyme in salicylate biosynthesis of *Pseudomonas aeruginosa*. *J. Biol. Chem.* 2003; 278:16893–16898. [PubMed: 12624097]
5. DeClue MS, Baldrige KK, Kunzler DE, Kast P, Hilvert D. Isochorismate Pyruvate Lyase: A Pericyclic Reaction Mechanism? *J. Am. Chem. Soc.* 2005; 127:15002–15003. [PubMed: 16248620]
6. Marti S, Andres J, Moliner V, Silla E, Tunon I, Bertran J. Mechanism and plasticity of isochorismate pyruvate lyase: a computational study. *J. Am. Chem. Soc.* 2009; 131:16156–16161. [PubMed: 19835359]
7. Luo Q, Olucha J, Lamb AL. Structure-function analyses of isochorismate-pyruvate lyase from *Pseudomonas aeruginosa* suggest differing catalytic mechanisms for the two pericyclic reactions of this bifunctional enzyme. *Biochemistry.* 2009; 48:5239–5245. [PubMed: 19432488]
8. Gustin DJ, Mattei P, Kast P, Wiest O, Lee L, Cleland WW, Hilvert D. Heavy Atom Isotope Effects Reveal a Highly Polarized Transition State for Chorismate Mutase. *J. Am. Chem. Soc.* 1999; 121:1756–1757.

9. Olucha J, Ouellette AN, Luo Q, Lamb AL. pH dependence of catalysis by *Pseudomonas aeruginosa* isochorismate-pyruvate lyase: Implications for transition state stabilization and the role of lysine 42. *Biochemistry*. 2011 in press.
10. Zaitseva J, Lu J, Olechowski KL, Lamb AL. Two crystal structures of the isochorismate pyruvate lyase from *Pseudomonas aeruginosa*. *J. Biol. Chem.* 2006; 281:33441–33449. [PubMed: 16914555]
11. Lee AY, Karplus PA, Ganem B, Clardy J. Atomic structure of the buried catalytic pocket of *Escherichia coli* chorismate mutase. *J. Am. Chem. Soc.* 1995; 117:3627–3628.
12. Liu DR, Cload ST, Pastor RM, Schultz PG. Analysis of Active Site Residues in *Escherichia coli* Chorismate Mutase by Site-Directed Mutagenesis. *J. Am. Chem. Soc.* 1996; 118:1789–1790.
13. Cload ST, Liu DR, Pastor RM, Schultz PG. Mutagenesis Study of Active Site Residues in Chorismate Mutase from *Bacillus subtilis*. *J. Am. Chem. Soc.* 1996; 118:1787–1788.
14. Chook YM, Gray JV, Ke H, Lipscomb WN. The monofunctional chorismate mutase from *Bacillus subtilis*. Structure determination of chorismate mutase and its complexes with a transition state analog and prephenate, and implications for the mechanism of the enzymatic reaction. *J. Mol. Biol.* 1994; 240:476–500. [PubMed: 8046752]
15. Chook YM, Ke H, Lipscomb WN. Crystal structures of the monofunctional chorismate mutase from *Bacillus subtilis* and its complex with a transition state analog. *Proc. Natl. Acad. Sci. U.S.A.* 1993; 90:8600–8603. [PubMed: 8378335]
16. Ladner JE, Reddy P, Davis A, Tordova M, Howard AJ, Gilliland GL. The 1.30 Å resolution structure of the *Bacillus subtilis* chorismate mutase catalytic homotrimer. *Acta Crystallogr.* 2000; D56:673–683.
17. Lee AY, Stewart JD, Clardy J, Ganem B. New insight into the catalytic mechanism of chorismate mutases from structural studies. *Chem. Biol.* 1995; 2:195–203. [PubMed: 9383421]
18. MacBeath G, Kast P, Hilvert D. Redesigning enzyme topology by directed evolution. *Science (New York, N.Y.)* 1998; 279:1958–1961.
19. Pervushin K, Vamvaca K, Vogeli B, Hilvert D. Structure and dynamics of a molten globular enzyme. *Nature structural & molecular biology.* 2007; 14:1202–1206.
20. Vamvaca K, Jelesarov I, Hilvert D. Kinetics and thermodynamics of ligand binding to a molten globular enzyme and its native counterpart. *Journal of molecular biology.* 2008; 382:971–977. [PubMed: 18680748]
21. Kast P, Asif-Ullah M, Jiang N, Hilvert D. Exploring the active site of chorismate mutase by combinatorial mutagenesis and selection: the importance of electrostatic catalysis. *Proc. Natl. Acad. Sci. U.S.A.* 1996; 93:5043–5048. [PubMed: 8643526]
22. Kast P, Grisostomi C, Chen IA, Li S, Krengel U, Xue Y, Hilvert D. A strategically positioned cation is crucial for efficient catalysis by chorismate mutase. *J. Biol. Chem.* 2000; 275:36832–36838. [PubMed: 10960481]
23. Kienhofer A, Kast P, Hilvert D. Selective stabilization of the chorismate mutase transition state by a positively charged hydrogen bond donor. *J. Am. Chem. Soc.* 2003; 125:3206–3207. [PubMed: 12630863]
24. Hur S, Bruice TC. The mechanism of catalysis of the chorismate to prephenate reaction by the *Escherichia coli* mutase enzyme. *Proc. Natl. Acad. Sci. U.S.A.* 2002; 99:1176–1181. [PubMed: 11818529]
25. Hur S, Bruice TC. The near attack conformation approach to the study of the chorismate to prephenate reaction. *Proc. Natl. Acad. Sci. U.S.A.* 2003; 100:12015–12020. [PubMed: 14523243]
26. Hur S, Bruice TC. Just a near attack conformer for catalysis (chorismate to prephenate rearrangements in water, antibody, enzymes, and their mutants). *J. Am. Chem. Soc.* 2003; 125:10540–10542. [PubMed: 12940735]
27. Hur S, Bruice TC. Comparison of formation of reactive conformers (NACs) for the Claisen rearrangement of chorismate to prephenate in water and in the *E. coli* mutase: the efficiency of the enzyme catalysis. *J. Am. Chem. Soc.* 2003; 125:5964–5972. [PubMed: 12733937]
28. Schowen RL. How an enzyme surmounts the activation energy barrier. *Proc. Natl. Acad. Sci. U.S.A.* 2003; 100:11931–11932. [PubMed: 14530397]

29. Zhang X, Zhang X, Bruice TC. A definitive mechanism for chorismate mutase. *Biochemistry*. 2005; 44:10443–10448. [PubMed: 16060652]
30. Andrews PR, Smith GD, Young IG. Transition-state stabilization and enzymic catalysis. Kinetic and molecular orbital studies of the rearrangement of chorismate to prephenate. *Biochemistry*. 1973; 12:3492–3498. [PubMed: 4731190]
31. Gajewski JJ, Jurayj J, Kimbrough DR, Gande ME, Ganem B, Carpenter BK. On the mechanism of rearrangement of chorismic acid and related compounds. *J. Am. Chem. Soc.* 1987; 109:1170–1186.
32. Claeysens F, Harvey JN, Manby FR, Mata RA, Mulholland AJ, Ranaghan KE, Schutz M, Thiel S, Thiel W, Werner HJ. High-accuracy computation of reaction barriers in enzymes. *Angew. Chem. Int. Ed.* 2006; 45:6856–6859.
33. Claeysens F, Ranaghan KE, Manby FR, Harvey JN, Mulholland AJ. Multiple high-level QM/MM reaction paths demonstrate transition-state stabilization in chorismate mutase: correlation of barrier height with transition-state stabilization. *Chem. Commun.* 2005:5068–5070.
34. Ranaghan KE, Mulholland AJ. Conformational effects in enzyme catalysis: QM/MM free energy calculation of the 'NAC' contribution in chorismate mutase. *Chem. Commun.* 2004:1238–1239.
35. Ranaghan KE, Ridder L, Szefczyk B, Sokalski WA, Hermann JC, Mulholland AJ. Transition state stabilization and substrate strain in enzyme catalysis: ab initio QM/MM modelling of the chorismate mutase reaction. *Org. Biomol. Chem.* 2004; 2:968–980. [PubMed: 15034619]
36. Luo Q, Olucha J, Lamb AL. Entropic and enthalpic components of catalysis in the mutase and lyase activities of *Pseudomonas aeruginosa* PchB. *J. Am. Chem. Soc.* 2011; 133:7229–7233. [PubMed: 21504201]
37. Harrison AJ, Yu M, Gardenborg T, Middleditch M, Ramsay RJ, Baker EN, Lott JS. The structure of MbtI from *Mycobacterium tuberculosis*, the first enzyme in the biosynthesis of the siderophore mycobactin, reveals it to be a salicylate synthase. *J. Bacteriol.* 2006; 188:6081–6091. [PubMed: 16923875]
38. Kerbarh O, Chirgadze DY, Blundell TL, Abell C. Crystal structures of *Yersinia enterocolitica* salicylate synthase and its complex with the reaction products salicylate and pyruvate. *J. Mol. Biol.* 2006; 357:524–534. [PubMed: 16434053]
39. Kerbarh O, Ciulli A, Howard NI, Abell C. Salicylate biosynthesis: overexpression, purification, and characterization of Irp9, a bifunctional salicylate synthase from *Yersinia enterocolitica*. *J. Bacteriol.* 2005; 187:5061–5066. [PubMed: 16030197]
40. Zwahlen J, Kolappan S, Zhou R, Kisker C, Tonge PJ. Structure and mechanism of MbtI, the salicylate synthase from *Mycobacterium tuberculosis*. *Biochemistry*. 2007; 46:954–964. [PubMed: 17240979]
41. Kolappan S, Zwahlen J, Zhou R, Truglio JJ, Tonge PJ, Kisker C. Lysine 190 is the catalytic base in MenF, the menaquinone-specific isochorismate synthase from *Escherichia coli*: implications for an enzyme family. *Biochemistry*. 2007; 46:946–953. [PubMed: 17240978]
42. Parsons JF, Shi KM, Ladner JE. Structure of isochorismate synthase in complex with magnesium. *Acta Crystallogr.* 2008; D64:607–610.
43. Sridharan S, Howard N, Kerbarh O, Blaszczyk M, Abell C, Blundell TL. Crystal structure of *Escherichia coli* enterobactin-specific isochorismate synthase (EntC) bound to its reaction product isochorismate: implications for the enzyme mechanism and differential activity of chorismate-utilizing enzymes. *J. Mol. Biol.* 2010; 397:290–300. [PubMed: 20079748]
44. Liu J, Quinn N, Berchtold GA, Walsh CT. Overexpression, purification, and characterization of isochorismate synthase (EntC), the first enzyme involved in the biosynthesis of enterobactin from chorismate. *Biochemistry*. 1990; 29:1417–1425. [PubMed: 2139795]
45. Ozenberger BA, Brickman TJ, McIntosh MA. Nucleotide sequence of *Escherichia coli* isochorismate synthetase gene *entC* and evolutionary relationship of isochorismate synthetase and other chorismate-utilizing enzymes. *J. Bacteriol.* 1989; 171:775–783. [PubMed: 2536681]
46. Daruwala R, Bhattacharyya DK, Kwon O, Meganathan R. Menaquinone (vitamin K2) biosynthesis: overexpression, purification, and characterization of a new isochorismate synthase from *Escherichia coli*. *J. Bacteriol.* 1997; 179:3133–3138. [PubMed: 9150206]

47. Knochel T, Ivens A, Hester G, Gonzalez A, Bauerle R, Wilmanns M, Kirschner K, Jansonius JN. The crystal structure of anthranilate synthase from *Sulfolobus solfataricus*: functional implications. *Proc. Natl. Acad. Sci. U.S.A.* 1999; 96:9479–9484. [PubMed: 10449718]
48. Ziebart KT, Toney MD. Nucleophile specificity in anthranilate synthase, aminodeoxychorismate synthase, isochorismate synthase, and salicylate synthase. *Biochemistry.* 2010; 49:2851–2859. [PubMed: 20170126]
49. Jackel C, Kast P, Hilvert D. Protein design by directed evolution. *Annu. Rev. Biophys.* 2008; 37:153–173. [PubMed: 18573077]
50. Lassila JK, Keefe JR, Kast P, Mayo SL. Exhaustive mutagenesis of six secondary active-site residues in *Escherichia coli* chorismate mutase shows the importance of hydrophobic side chains and a helix N-capping position for stability and catalysis. *Biochemistry.* 2007; 46:6883–6891. [PubMed: 17506527]
51. Benkovic SJ, Hammes GG, Hammes-Schiffer S. Free-energy landscape of enzyme catalysis. *Biochemistry.* 2008; 47:3317–3321. [PubMed: 18298083]

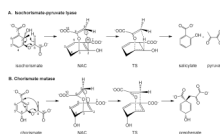


Figure 1. Pericyclic reactions catalyzed by PchB

A. Isochorismate-pyruvate lyase: hydrogen transfer from C2 to C9 concerted with pyruvate elimination. B. Chorismate mutase: C-C bond formation between C1 and C9 concerted with C-O bond fission between C3 and the ether oxygen.

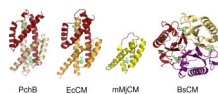


Figure 2. Structure of PchB, *E. coli* chorismate mutase, monomeric *Methanococcus jannaschii* chorismate mutase and *B. subtilis* chorismate mutase

The PchB dimer is shown in red and tan with salicylate and pyruvate shown in green sticks (PDB code: 3REM). The EcCM dimer is red and gold with the oxabicyclic transition state analogue (TSA) in green sticks (PDB code: 1ECM). The mMjCM monomer is shown in yellow with the inserted intrahelical turn shown in red and the TSA in green (PDB code: 2GTV). The BsCM dimer is red, yellow and magenta with the TSA in green (PDB code: 2CHS).

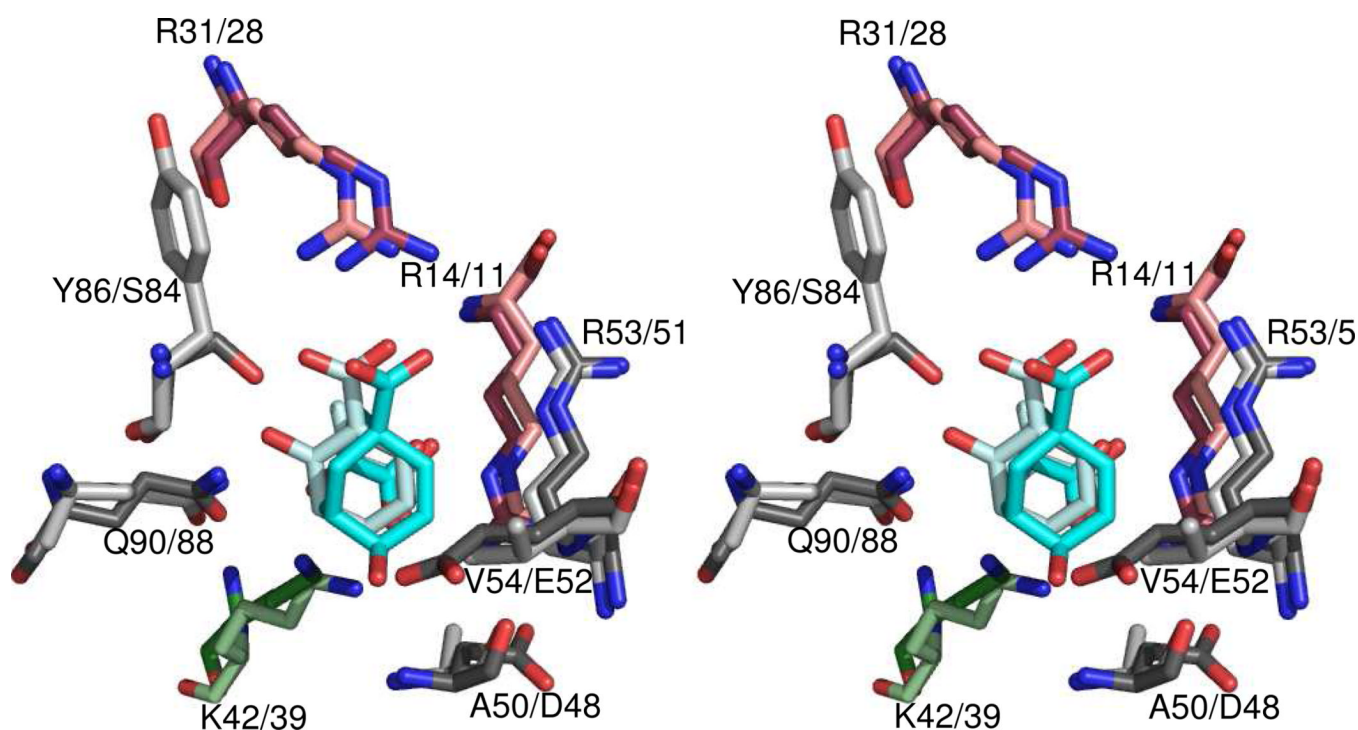


Figure 3. Stereo image comparing the active site of PchB and EcCM

The arginines that align the carboxylates of the substrate are shown in pink, and the lysine hypothesized to be important in the transition state stabilization theory is shown in green. The ligands are shown in cyan: salicylate and pyruvate in the PchB structure and TSA in the EcCM structure. In all cases, the lighter shades are PchB and darker are EcCM. Amino acids are labeled as PchB numbering/EcCM numbering.

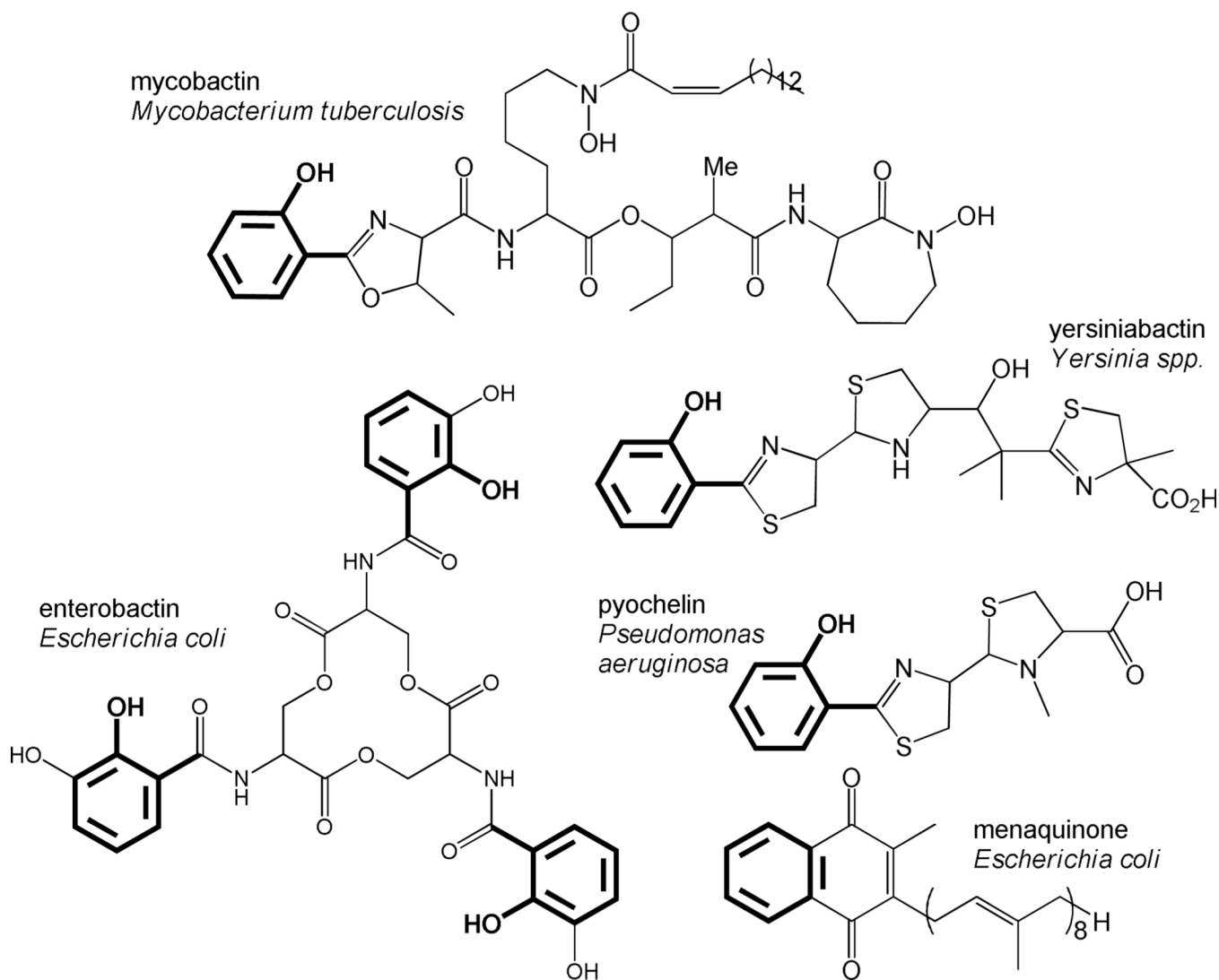


Figure 4. Biosynthetic products

All of the above compounds require the conversion of chorismate to isochorismate as a part of their biosynthesis. The portion of the compound that is derived from the isochorismate is shown in bold. Mycobactin, yersiniabactin and pyochelin are salicylate-capped siderophores. Enterobactin is also a siderophore, capped by di-hydroxybenzoate. Menaquinone is an electron carrier and a form of Vitamin K.

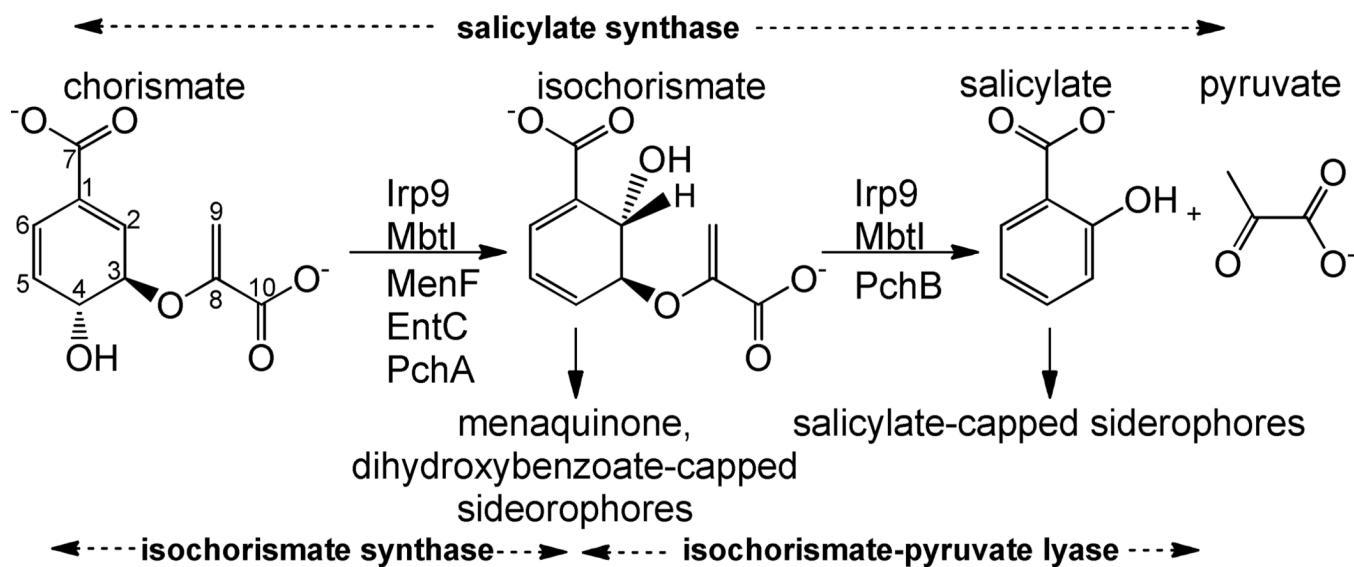


Figure 5. Reactions catalyzed by isochorismate and salicylate synthases

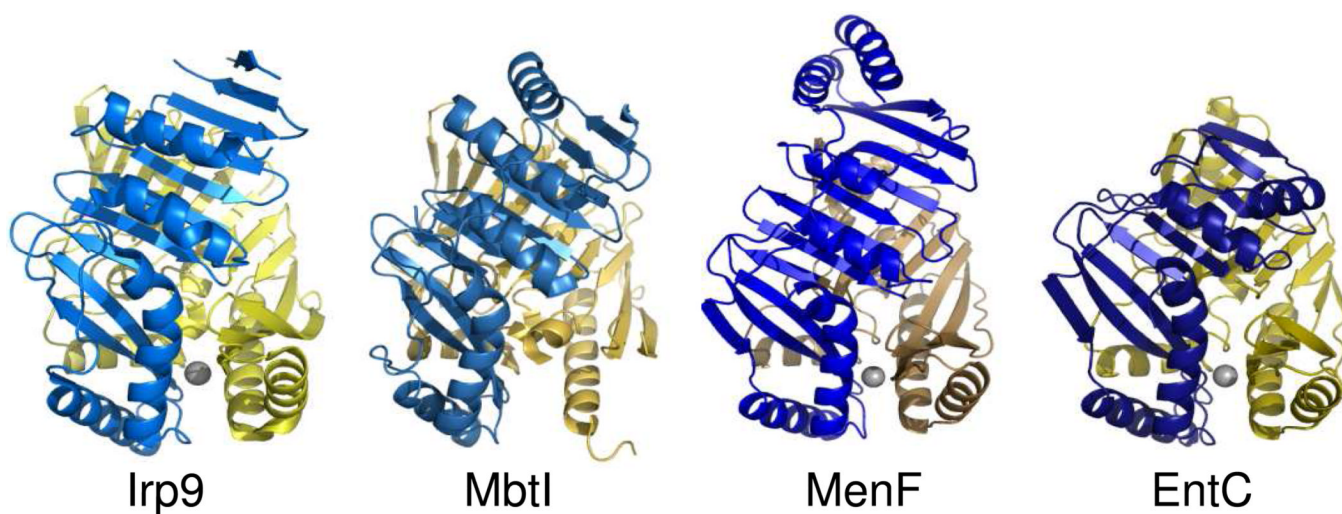


Figure 6. Structures of the salicylate synthases (Irp9 and MbtI) and isochorismate synthases (MenF and EntC)

The domains of these monomeric proteins are shown as blue and yellow. Mg^{2+} , if in determined structures, are shown as gray spheres. (PDB codes: Irp9 – 2FN1, MbtI – 2I6Y, MenF – 2BZM, EntC – 3HWO).

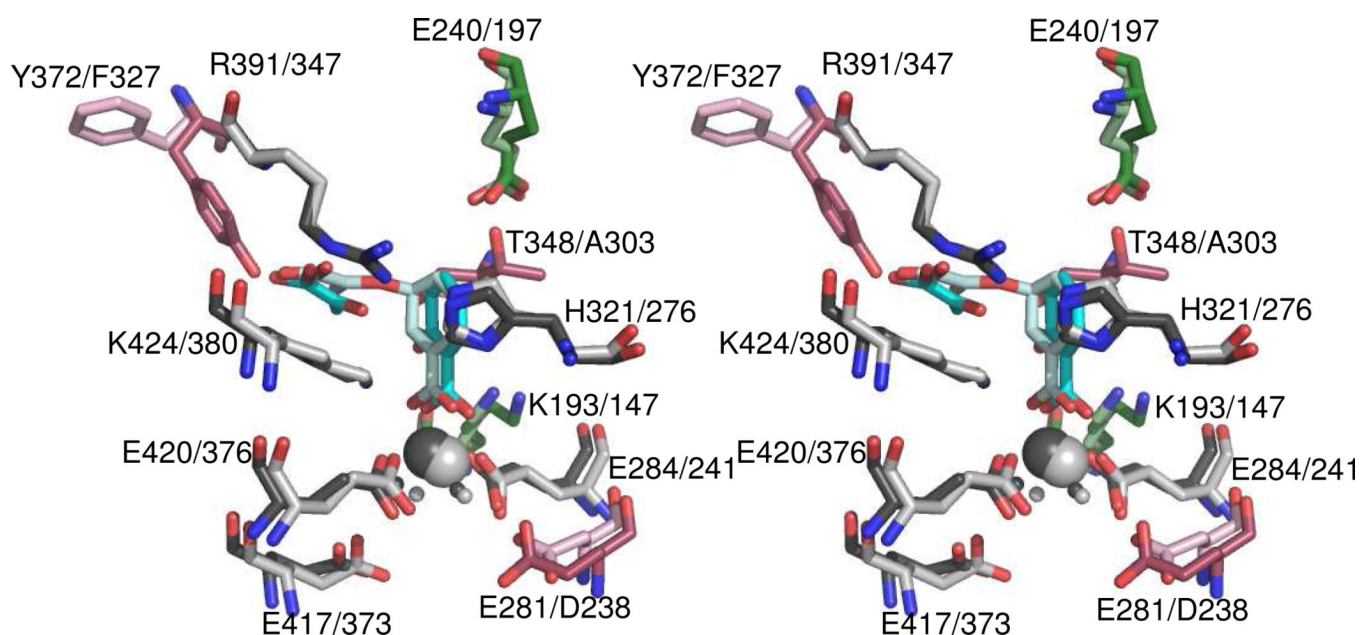


Figure 7. Stereo image comparing the active sites of Irp9 and EntC

The general acid/general base residues are shown in green, and Mg^{2+} is shown as a sphere. Non-conserved residues are pink. Ligands are shown in cyan: salicylate and pyruvate in the Irp9 structure and isochorismate of the EntC structure. In all cases, the lighter shades are EntC and darker are Irp9. Amino acids are labeled as Irp9 numbering/EntC numbering.

Table 1

Function of active site amino acids in isochorismate and salicylate synthases (residues chosen based on Irp9 structure¹ with Mg⁺², salicylate and pyruvate bound)

Residue function	general base for ICS activity	general acid for ICS activity	chelate Mg ⁺² thru H ₂ O	chelate Mg ⁺²	backbone carbonyl H-bonds to salicylate or isochor. OH	orients pyruvyl carbonyl	orients pyruvyl carbonyl	chelate Mg ⁺² thru H ₂ O	chelate Mg ⁺²	positive charge for pericyclic IPL activity?
Irp9 ¹	K193	E240	E281	E284	T348	Y372	R391	E417	E420	K424
MbtI ³	K205	E252	E294	E313	T361	Y385	R405	E431	E434	K438
MenF ³	K190	E240	N281	E284	A344	Y368	R387	E413	E416	K420
EntC ⁴	K147	E197	D238	E241	A303	F327	R347	E373	E376	K380
PchA	K221	E269	D310	E313	A375	Y399	R419	E445	E448	K452

¹ Irp9 data from Kerbarth *et al.* (ref ref 38)

³ MbtI data from Harrison *et al.* (ref ref 37) and Zwahlen *et al.* (ref 40)

³ MenF data from Kolappan *et al.* (ref 41) and Parsons *et al.* (ref 42)

⁴ EntC data from Sridharan *et al.* (ref 43)